Analysis of the relationship between MCC and thermal analysis results in evaluating flammability of EPS foam

Qiang Xu · Cong Jin · Yong Jiang

Abstract The thermal properties of EPS foam were tested by simultaneous thermal analysis in a nitrogen environment, using a Netzsch STA 449C TG-DSC. Pyrolysis products were characterized using mass spectrometry and Fourier transform infrared spectroscopy. The flammability of EPS foam was examined using microscale combustion calorimetry. Heat release rate, peak heat release rate, heat release capacity, and some typical temperatures were obtained. The relationships between thermal analysis and MCC were derived from above test results. This could become a significant methodology in establishing the parameters contributing to flammability of polymers.

Keywords Microscale combustion calorimetry (MCC) · Flammability · Expanded polystyrene foam · Simultaneous thermal analysis · Decomposition

Introduction

The essential characteristics that describe quantitatively "how big is the fire" is the heat release rate (*HRR*) [1]. It is widely used flammability assessment and for describing the

Q. Xu (✉)
School of Mechanical Engineering, Nanjing University of Science and Technology, Nanjing 210014, China
e-mail: kentqxu@hotmail.com

C. Jin
School of Computer Science and Technology, Nanjing University of Science and Technology, Nanjing 210014, China

Y. Jiang
State Key Laboratory of Fire Science, University of Science and Technology of China, Hefei 230026, China

fire behavior of material [2]. *HRR* can be measured using the technique of "oxygen consumption" calorimetry. This can be determined using different scale calorimeters, such as the ISO 9705 room scale test, the ISO5660 bench scale cone calorimeter, and the microscale combustion calorimeter (MCC) ASTM D7309-07 [3], in which HRR can be obtained using the conversion factor 13.1 kJ g^{-1} of oxygen consumed. Prediction of HRR by modeling of the pyrolysis process has drawn great interest in flammability research. This is often described as creating a pyrolysis model because the degradation of material when it is exposed to heat is known as pyrolysis. When a material heats up, it may degrade to generate fuel fragments which ignite and burn. Complicated physical and chemical phenomena take place [1].

To discover the effect of material properties and composition on burning behavior, a quantitative analytical laboratory test that correlates fire behavior or flame test performance with material properties has been developed to relate the results of thermogravimetric analysis to flammability [4]. Microscale combustion calorimetry (MCC) or pyrolysis-combustion flow calorimetry (PCFC) has been developed for this purpose. Unlike thermogravimetric investigations of flammability which have relied on a single thermal stability parameter, in MCC, the pyrolysis products generated from a controlled pyrolysis in an inert gas stream are mixed with excess oxygen and combusted (oxidized) at high temperature, and the instantaneous heat of combustion of the flowing gas stream is measured by oxygen consumption calorimetry [4]. Results from MCC are not dependent on ignition source, sample thickness and orientation, ventilation, or edge condition in bench, and room scale tests [4]. The correlation of MCC parameters with conventional flammability tests such as LOI, UL 94, and cone calorimetry has been investigated [5]. Results from MCC have been compared with those from TG-gas chromatography/mass
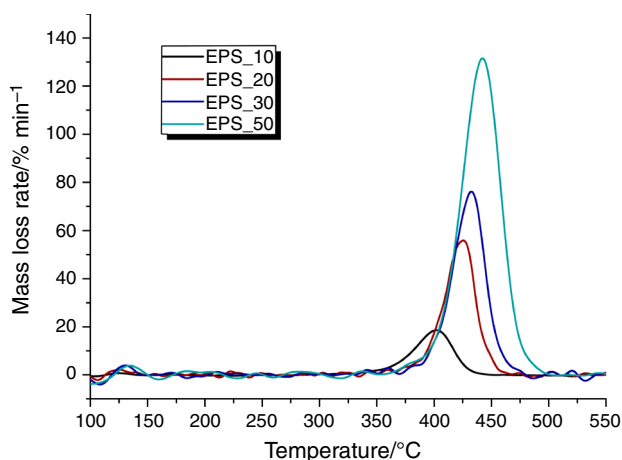
spectrometry, oxygen bomb calorimetry, and cone calorimetry for selected polymers [4]. MCC was established as an international standard test method in 2007 [3] [6]. Since then MCC has been used in material flammability research, especially in fire retardant research [7–10].

EPS foam panel is one end-use product of expandable polystyrene. Foam products typically are more sensitive to heat than their solid equivalents [11]. EPS is flammable; thus, the principal safety hazard of EPS foam panel is fire. Many large scale tests have been utilized to characterize the fire behavior of EPS [12–15]. The flammability of EPS has been evaluated using multi-scale methods [16]. In this approach, TG, DSC, cone calorimetry, and real-scale fire testing were used. MCC was adopted for further study. Results from MCC may be correlated with results from previous simultaneous thermal analysis. With the aid of mass spectrometry and Fourier transform infrared spectroscopy, the process from pyrolysis to combustion may be better understood.

Test descriptions

Test facilities

The experiments were carried out by means of STA (Simultaneous Thermal Analysis, using a Netzsch STA 449C TG-DSC) which applies thermogravimetry (TG) and differential scanning calorimetry (DSC) to EPS foam samples under a nitrogen atmosphere. A heating rate of 10, 20, 30, and 50 °C min^{-1} from 50 °C to a maximum temperature of 600 °C was used with a gas flow rate of 75 mL min^{-1}. Samples were contained in Al_2O_3 crucibles without lids.

Coupled techniques, such as STA-FTIR-MS, that enable the identification of the gases that are evolved during EPS pyrolsis were used in this research. The STA was coupled to evolved gas analysis (EGA) detectors. The pyrolysis products from STA were examined using mass spectrometry (MS), using a type QMS403C unit from Netzsch, and Fourier transform infrared spectroscopy (FTIR), using a type 5700 instrument from Nicolet Instrument Company. For FTIR, the wavenumber range was set as 4,000–400 cm^{-1}. MS and FTIR measurement were coupled with STA at heating rate of 10 and 50 °C min^{-1}.

MCC tests were conducted on Type MCC-2, from Govmark Organization, Inc., Farmingdale, NY, USA, according to the ASTM standard test method D7309-2007, using 'Method A' [3]. The heating rate was 10, 20, 30, 50, and 100 °C min^{-1}.

EPS foam was from Jiangsu Sanyou Plastics Co., Ltd. The foam has a density of 8.033 kg m^{-3} and a normal level of fusion. A molecular mass determination for the foam was not performed. A LOI test carried out according to ASTM D2863 provided a value of 22.2.
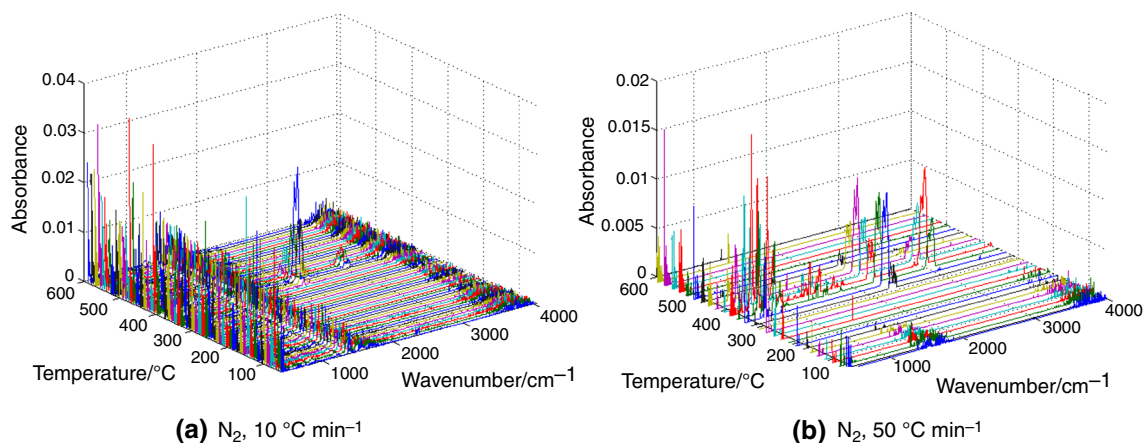
Test results

STA, FTIR, and MS test results

Illustrative DTG curves are presented in Fig. 1. There is only one degradation stage for EPS. A delay in degradation and a shift of the curves to higher temperatures with increasing heating rate were observed in agreement with previous observations [17], [18]. At lower heating rates, the sample spends a longer time at a certain temperature; thus, more degradation will occur before the sample reaches the next temperature zone [18]. The conversion reaches its

Fig. 1 DTG curves

Table 1 Typical data obtained from TG curve

Sample label	T_5/°C	T_{50}/°C	T_{95}/°C	TR_{max}/°C	Conversion/%	Peak conversion rate vs. Time/% min^{-1}
EPS_10	351	397	422	402	61.3	23.0
EPS_20	381	421	447	427	65.3	55.7
EPS_30	393	429	455	432	57.7	79.4
EPS_50	407	441	464	443	57.1	140.2

T_5 temperature of 5 % sample mass loss, T_{50} temperature of 50 % sample mass loss, T_{95} temperature of 95 % sample mass loss, TR_{max} temperature of sample thermal decomposition maximum rate

Table 2 Typical data obtained from DSC

Sample label	Inflection temperature of glass transition/°C	Peak temperature for a endothermic event/°C	Temperature range for the of endothermic effect/°C	Enthalpy/J g^{-1}
EPS_10	132.4	404	361–423	2407
EPS_20	122.2	426	376–474	1476
EPS_30	132.3	438	378–484	728
EPS_50	135.0	450	391–521	602

(a) N$_2$, 10 °C min^{-1} (b) N$_2$, 50 °C min^{-1}

Fig. 2 FTIR spectra of degradation products evolved from TG

peak rate between 57.1 and 65.3 %. The conversion rate is greater for 50–90 % conversion than for 5–50 % conversion as shown in Table 1. In DTG curves, there is a small fluctuation at different heating rates at around 125 °C. This is due to air which escapes from the foam cell when it breaks.

Only one main endothermic event is observed in the DSC curve for each sample. This event occurs at temperature greater than 350 °C. The peak temperature for the endothermic event shifts to higher temperature as the heating rate increases. This behavior, in an inert environment, is similar to that previously described [19]. Typical data obtained from DSC are listed in Table 2.

The 3D FTIR spectra of degradation products obtained from thermal degradation at 10 and 50 °C min^{-1} heating rates in a nitrogen atmosphere are shown in Fig. 2. A detailed analysis of the spectra suggests the following results.

At 372.5 °C, it begins to produce CO_2 (fundamental frequency absorption peak at 669 and 2,349 cm^{-1}), single substituted benzene (out-of-plane ring bend vibrations at 669 and 2,349 cm^{-1}, planar aromatic skeleton vibrations ranging from 1,430 to 1,600 cm^{-1}), m-di-substitution benzene (three absorption peaks located at 695, 771 and 900 cm^{-1}), alkynes (C≡C symmetric stretching vibration nearby 2,309 and 2,380 cm^{-1}), H_2O (from 3,500 to 4,000 cm^{-1}). There may be some acids, esters, and ethanol

(CO stretching vibration nearby 1,217 cm^{-1}, carbonyl stretch vibration at 1,650 to 1,900 cm^{-1}). With the temperature increasing, more substances are generated. When it reaches the maximum mass loss velocity temperature at 404.2 °C, the amount of resultant reached maximum. In addition to above compounds, it produces terminal olefins (the out-of-plane of CH bending mode nearby 910 and 990 cm^{-1}, CH stretching vibration at 3,072 cm^{-1}, C=C symmetric stretching vibration at 1,500 to 1,680 cm^{-1}). Then, considering the absorption peaks centering at 695 and 719 cm^{-1}, this kind of terminal olefins can be adjudged to be styrene.

With further increase of temperature, the amount of resultant decreases and eventually stops generating. Although terminal olefins increase very slowly in early stage, it has a sharp decrease in the latter period. Above all, at initial period of degradation, it mainly produces some styrene polymers, whereas the generation of other resultant is caused for oxidation. As temperature further increased, the amount of styrene reaches maximum at maximum mass loss velocity. In conclusion, during pyrolysis of EPS at nitrogen atmosphere, weak bond begins to break randomly, then polymers further degrades after initial pyrolysis until all polymers degrades to styrene monomer; thus, the pyrolysis mechanism of EPS is mainly random degradation.

Figure 3a is the variation diagram that ion current density varies with temperature with heating rate of

(b) N_2, 10° C min^{-1}

(b) N_2, 50 °C min^{-1}
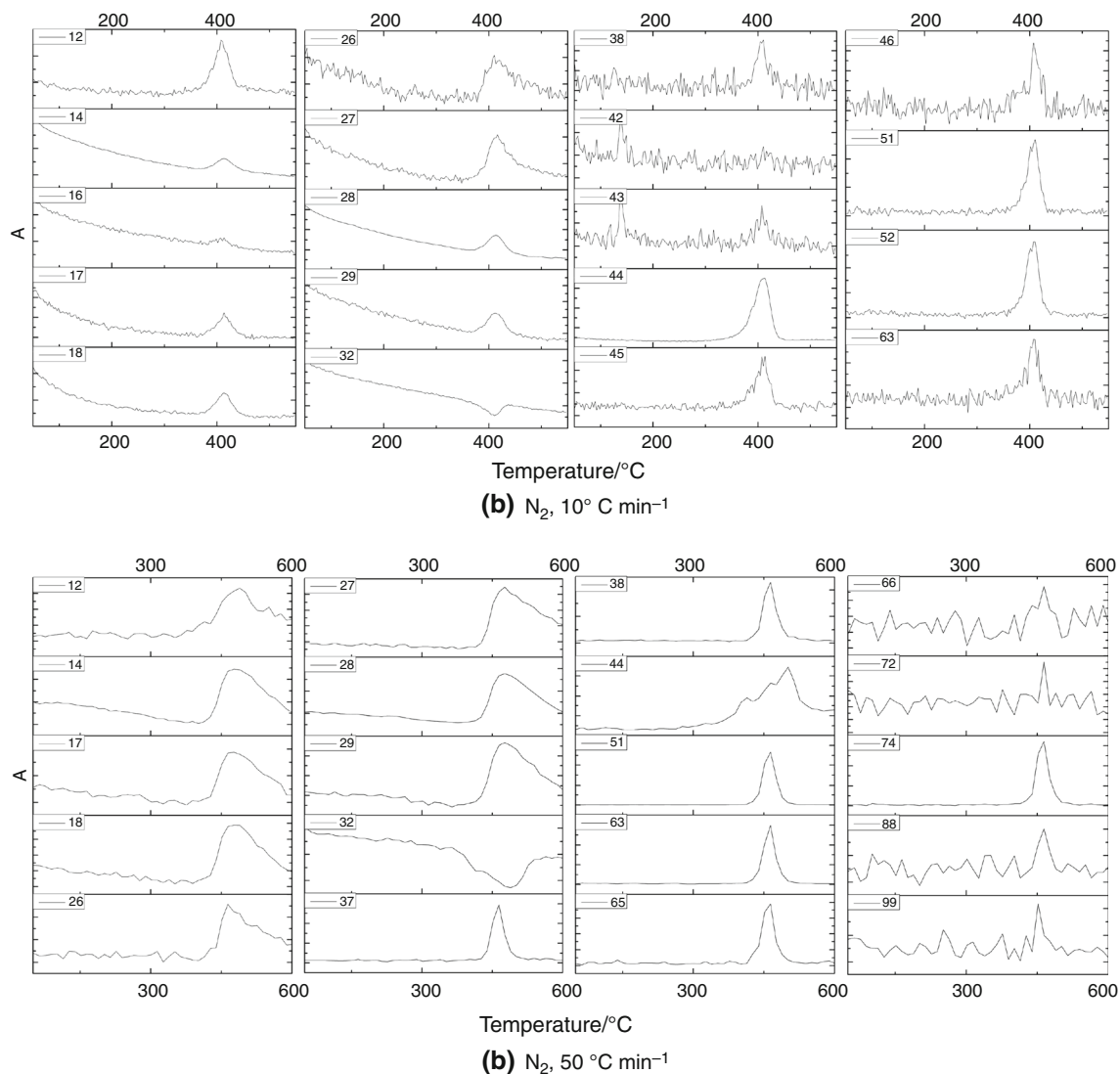
Fig. 3 MS results

10 °C min^{-1} at a nitrogen atmosphere. m/z detected by MS and the temperature range are listed in Table 3. m/z 42 was detected from 125 to 150 °C, which accorded with glass-transition temperature measured by DSC. Meanwhile, an absorption peak from 2300 to 2,500 cm^{-1} is found in 3D infrared spectra (Fig. 2); thus, it can be judged as propylene, which may be produced after the foaming agent rupture. The ion current density of m/z 32 decreases from 375 to 445 °C, which may be caused by the reduction of oxygen mingled in a nitrogen atmosphere.

According to the above infrared spectra, it can be defined that m/z 14, 16, 26, 27, 29, 38, 43, 51, 52, 63 are some alkane, olefin hydrocarbons, and alkyne. The maximum ion current density accords with maximum mass loss velocity. m/z 28 may be CO, which is the resultant of EPS and oxygen impurity.

m/z 18 is H_2O, which can be verified from 3,500 to 4,000 cm^{-1} on the infrared spectra. m/z 44 may be CO_2 or C_3H_8, and then we can identify, it is CO_2 by the absorption peak at 669 and 2,349 cm^{-1} in infrared spectra. m/z 12 is C, and m/z 45 is C_2H_5O, then we can deduce, it is CH_2CH_2OH by the IR spectra. m/z 46 is C_2H_6O or CH_2O_2, and it may be CH_3CH_2OH (HO stretching vibration at 3,000 to 3,750 cm^{-1}) or HCOOH (CO stretching vibration at 1,217 cm^{-1}, carbonyl stretching vibration nearby 1,650 to 1,900 cm^{-1}).

From the above analysis, a conclusion could be drawn that the pyrolysis products of EPS in nitrogen atmosphere mainly contain some micromolecules, such as single substituted, m-di-substitution benzene, alkane, olefin hydrocarbons, alkyne, CO, H_2O, C, CO_2, and ethyl alcohol.

When the temperature rises up to 443 °C, it also generates m-di-substitution benzene and terminal olefins in

Table 3 MS results

m/z (β = 10 °C min^{-1})	T/°C (β = 10 °C min^{-1})	m/z (β = 50 °C min^{-1})	T/°C (β = 50 °C min^{-1})	Possible ions
12	375–445	12	420–600	C
14	375–445	14	420–600	CH_2, N
16	375–445	–	–	CH_4, O
17	375–445	17	420–600	OH
18	375–445	18	420–600	H_2O
26	375–445	26	420–600	C_2H_2
27	375–445	27	420–600	C_2H_3
28	375–445	28	420–600	C_2H_4, CO, N_2
29	375–445	29	420–600	C_2H_5
32	375–445	32	375–550	O_2
–		37	420–500	C3H
38	375–445	38	420–500	C_3H_2
42	125–150	–	–	C_3H_6, C_2H_2O
43	125–150, 375–445	–	–	C_3H_7, C_2H_3O
44	350–445	44	400–550	CO_2, C_3H_8, C_2H_4O
45	375–445	–	–	C_2H_5O, CHO_2
46	375–445	–	–	C_2H_6O, CH_2O_2
51	375–445	51	420–500	C_4H_3
52	375–445	–	–	C_4H_4
63	375–445	63	420–500	CH_3O_3, C_5H_3
–	–	65	420–500	C_4HO, C_5H_5
–	–	66	420–500	C_4H_2O, C_5H_6
–	–	72	420–500	C_4H_8O, C_5H_{12}
–	–	74	420–500	$C_2H_2O_3$, $C_3H_6O_2$, C_6H_2
–	–	88	420–500	$C_4H_8O_2$, $C_5H_{12}O$, C_7H_4
–	–	99	420–500	$C_5H_7O_2$, $C_6H_{11}O$

addition to above substance. As the temperature increases, these products disappear gradually, this tendency is similar to the situation at 10 °C min^{-1}. However, there are some differences at the m-di-substitution benzene generated temperature between both heating rates.

Figure 3b is the mass spectra at the heating rate of 50 °C min^{-1}. Details of temperature range and possible ions are also listed in Table 3. According to Table 3 and above infrared analysis, we can obtain that m/z 12, 14, 17, 18, 26, 27, 29 are C, alkane, olefin hydrocarbons, and alkyne, respectively.

These micromolecules can be detected ranging from 420 to 600 °C, which indicated that these fragments ions are generated even at the end stage of pyrolysis. m/z 28 is CO detected from 420 to 600 °C through the whole pyrolysis process, and m/z 44 is CO_2, whereas its detected temperature range is 420 to 550 °C, which is narrower than the former. O_2 (m/z = 32) is detected ranging from 375 to 550 °C at the heating rate of 50 °C min^{-1}, which is the same with the mass spectra of 10 °C min^{-1}.

This phenomenon means that oxygen participates in reaction at the initial phase of pyrolysis. m/z 37, 38, 51, 63,

65, 66 are fragment ions of alkane, olefin hydrocarbons, and alkyne. And its temperature range is 420 to 500 °C, which is shorter than those small mass charge ratio ions. So, it can be deduced that these small mass charge ratio ions come from further degradation of large mass charge ratio ions. As to even larger mass charge ratio ions, for example, m/z 72, 74, 88, 89, all these may be the fragment ions of alkane, olefin hydrocarbons, and alkyne, of course, it also may be of alcohol or acid.

By FTIR and MS analysis at different heating rates (10 and 50 °C min^{-1}), we can conclude that the pyrolysis mechanism of EPS in nitrogen atmosphere is random pyrolysis, and the degradation products at two different heating rates are similar, including single substituted (styrene),m-di-substitution benzene, alkane, olefin hydrocarbons, alkyne, acid, CO, O, CO_2, and alcohol.

Main generated products were accordance with respective mass loss temperature. The mass spectra of 50 °C min^{-1} can detect both small and large mass charge ratio ions, whereas 10 °C min^{-1} mass spectra only showed the small mass charge ratio ions. This difference is explained by the fact that it is too short for large ions to

(a) Heat release rate
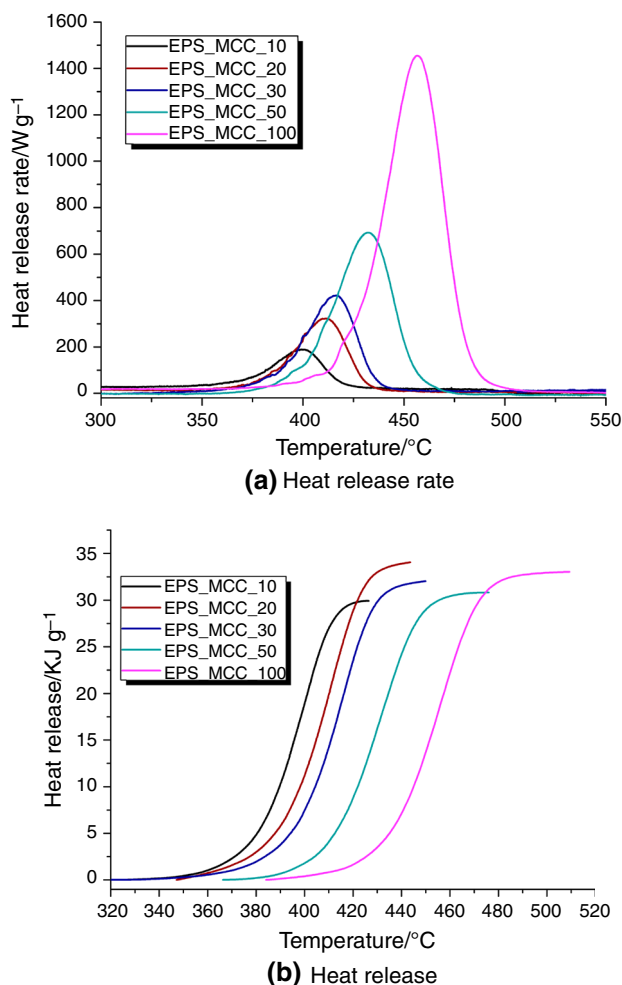
(b) Heat release

Fig. 4 MCC results

break into small ions, on the contrary, for the case of 10 °C min^{-1}, large ions have enough time to break into small ones.

MCC test results

The parameters used to characterize flammability can be examined using MCC are heat release capacity (*HRC*, J g^{-1} °C^{-1}), heat, release rate (*HRR*, W g^{-1}) at different temperatures, peak heat release rate (*pHRR*, W g^{-1}), temperature at *pHRR* (T_{pHRR}, °C), and total heat release (*THR*, kJ g^{-1}). HRC, which is obtained by dividing the maximum value of the specific heat release rate (*SHRR*) with the heating rate (°C s^{-1})in the test, is a material property [4]. It appears to be a good predictor of flammability and propensity for ignition, and it is related to the decomposition kinetics and combustion parameters of the sample [4]. Swelling and dripping of thermoplastics influence flame fire tests, such as cone calorimeter test, but do not affect *HRC*.
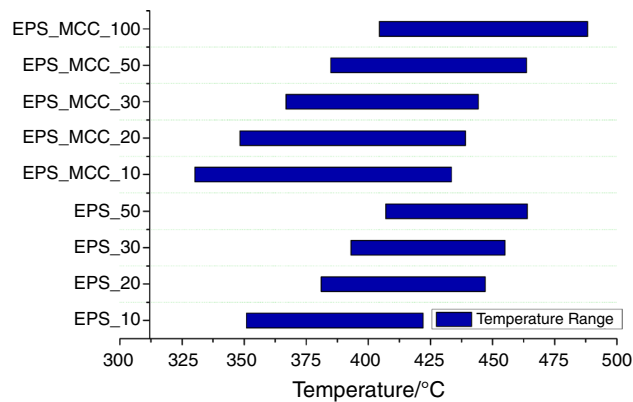
Fig. 5 Temperature ranges of mass loss and non-flame combustion

Table 4 Typical data obtained from MCC

Sample label	HRC/ J g^{-1} °C^{-1}	pHRR/ W g^{-1}	THR/ kJ g^{-1}	T_{pHRR}/ °C	T_{up5}/ °C	T_{down5}/ °C
EPS_MCC_10	1136.4	189.4	29.9	399.2	330.1	433.5
EPS_MCC_20	968.4	322.8	34.0	411.6	348.3	439.1
EPS_MCC_30	844.8	422.4	32.1	415.6	366.9	444.3
EPS_MCC_50	831.7	693.1	30.8	432.2	384.8	463.7
EPS_MCC_100	873.0	1454.9	33.0	457.0	404.5	488.3

T_{pHRR} temperature of peak heat release rate, T_{up5} temperature of 5 % peak heat release rate in rising stage, T_{down5} temperature of 5 % of peak heat release rate in declining stage

HRR versus time curves are shown in Fig. 4a, T_{pHRR} shifts to higher temperature with increasing heating rate as the DTG curves. The groups of *HRR* curves have the same shape and tendency as TG and DTG (shown in Fig. 1a, b). Typical parameters are listed in Table 4. *HRC* decreases with increase of heating rate generally, except for 100 °C min^{-1}. *pHRR* increases with increase of heating rate. The range of *THR* is from 29.9 to 34.0 kJ g^{-1}, shown in Fig. 4b and Table 4. Temperature ranges of *HRR* in MCC and mass loss in STA are shown in Fig. 5.

Conclusions

The more pyrolyzate produced per unit of time, the more heat release rate generated in forced combustion. This is the main reason account for high *pHRR* appearing at high heating rate.

This suggests that HRR depends on heating rate in MCC tests. MCC can be used to characterize the fundamental performance of materials in forced combustion condition. The forced combustion condition is quite different from real fire scenario; thus, results from MCC cannot be used to modeling or predicting fire behavior of materials directly. High heating rate MCC test would be more helpful in

understanding material's combustion performance, while in STA test low heating rate would be helpful in analyzing pyrolyzate.

HRC decreases with the increase of heating rate, while the total heat release is independent of heating rate. It is the sum of heat release from all combustibles when forced to combust in MCC, and it assumed to have the same value even at different heating rates. It could be used as a measure of combustion potential of materials and used to compare fire hazard potential among materials.

There is no direct corresponding relationship between MCC and DSC data, such as the *pHRR* in MCC and endothermic peak in DSC, except for typical temperature ranges are the same. In the tests presented above, the temperature of *pHRR* in MCC is lower than peak temperature in DTG and DSC at every heating rate, but the differences are not significant, within systematic errors of both equipments.

From the comparison of typical temperature ranges from MCC to DTG, the temperature at which *HRR* reaches 5 % of *pHRR* in MCC is lower than the temperature at which mass loss reaches 5 % in DTG. It partly implies that the pyrolyzate in early stage contributes more to *HRR*.

From MS and FTIR results at 10 and 50 °C min^{-1} heating rate, EPS decomposes more sufficiently at low heating rate. At low heating rate, the amount of pyrolyzate swept into combustion furnace is less than that at high heating rate, and almost of pyrolyzates are smaller fragment than those at high heating rate. At high heating rate, bigger fragments in combustion chamber further decompose and combust, more oxygen is consumed than at low heating rate, it will cause a higher *pHRR*. It is the main reason that HRR depends on heating rate in MCC tests.

References

1. The SFPE Handbook of Fire Protection Engineering, Third Edition, ISBN: 087765-451-4.
2. Lindholm Johan, Brink Anders, Hupa Mikko. Influence of decreased sample size on cone calorimeter results. Fire Mater. 2012;36:63–73.
3. Standard test method for determining flammability characteristics of plastics and other solid materials using microscale combustion calorimetry, ASTM 7309–07. American Society for Testing and Materials (International), West Conshohocken, PA (1 April 2007).
4. Richard E. Lyon and Richard Walters. A Microscale Combustion Calorimeter. DOT/FAA/AR-01/117. Feb 2002.
5. Thomas S. Lin, Jeffrey M. Cogen, Richard E. Lyon. Correlations between Microscale Combustion Calorimetry and Conventional Flammability Tests for Flame Retardant Wire and Cable Compounds, Proceedings of the 56th International Wire & Cable Symposium, 2007.
6. Yang CQ, He Q. Textile heat release properties measured by microscale combustion calorimetry: experimental repeatability. Fire Mater. 2012;36:127–37.
7. Chen LJ, Tai QL, Song L, Xing WY, Jie GX, Hu Y. Thermal properties and flame retardancy of an ether-type UV-cured polyurethane coating. eXPRESS Polym Lett. 2010;4(9):539–50.
8. Yang CQ, He Q. Applications of micro-scale combustion calorimetry to the studies of cotton and nylon fabrics treated with organophosphorus flame retardants. J Anal Appl Pyrol. 2011;91:125–33.
9. Shuang Hu, Song Lei, Pan Haifeng, Yuan Hu. Effect of a novel chitosan-based flame retardant on thermal and flammability properties of polyvinyl alcohol. J Therm Anal Calorim. 2013;112(2):859–64.
10. Howell BA, Dumitrascu A. Thermal and combustion characteristics of phosphorus and phosphorus/nitrogen-containing styrene monomers and oligomers. J Therm Anal Calorim. 2012;109(3):1133–7.
11. Expandable Polystyrene Storage and Handling Safety Guide. NOVA Chemicals Corporation. 2005.
12. Benrashid Ramazan, Nelson GordonL, Ferm DonaldJ. Effect of Triaryl Phosphate, Zinc and Zinc Borate on Fire Properties of High Impact Polystyrene and High Impact Polystyrene-Polyphenylene Oxide Blend (Modified-Polyphenylene Oxide). J Fire Sci. 1994;12:529–50.
13. Xie Qiyuan, Zhang Heping, Ye Ruibo. Experimental study on melting and flowing behavior of thermoplastics combustion based on a new setup with a T-shape trough. J Hazard Mater. 2009;166:1321–5.
14. Zhang Ying, Huang Xinjie, Wang Qingsong, Ji Jie, Sun Jinhua, Yin Yi. Experimental study on the characteristics of horizontal flame spread over XPS surface on plateau. J Hazard Mater. 2011;189:34–9.
15. Griffin GJ, Bicknell AD, Bradbury GP, White N. Effect of construction method on the fire behavior of sandwich panels with expanded polystyrene cores in room fire tests. J Fire Sci. 2006;24:275–94.
16. Qiang Xu, Cong Jin, Greg Griffin, Yong Jiang. Fire safety evaluation of expanded polystyrene foam by multi-scale methods. J Therm Anal Calorim. doi: 10.1007/s10973-013-3431-6.
17. Azimi HamidReza, Rezaei Mostafa, Abbasi Farhang. Thermooxidative degradation of MMA–St copolymer and EPS lost foams: kinetics study. Thermochim Acta. 2009;488:43–8.
18. Kannan Pravin, Biernacki JosephJ, Visco DonaldP Jr, Lambert William. Kinetics of thermal decomposition of expandable polystyrene in different gaseous environments. J Anal Appl Pyrol. 2009;84:139–44.
19. Dauengauer SA, Utkina OG, Popova GS, Sazanov YuN. Investigation of thermal degradation of polystyrene with the aid of thermal analysis. J Therm Anal Calorim. 1987;32:311–4.